

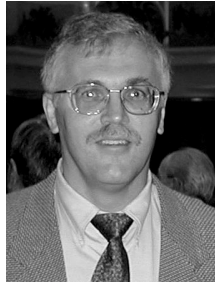
An Analysis of Maneuvering Effects on Transmission Vibrations in an AH-1 Cobra Helicopter



Edward M. Huff
Senior Scientist



Irem Y. Tumer
Research Scientist



Eric Barszcz
Research Scientist



Mark Dzwonczyk
President



James McNames¹
Signal Analyst

Computational Sciences Division
NASA Ames Research Center
Moffett Field, CA 94035-1000

Sigpro
Mountain View, CA 94041

During the past several years, an AH-1 Cobra aircraft at the NASA Ames Research Center has been instrumented with tri-axial accelerometers and a data acquisition system to support the experimental study of in-flight transmission vibration patterns. This paper describes the on-board *HealthWatch* system and presents important statistical analyses of the collected data sets. These analyses provide insight into how transmission vibration responds to several factors typically related to health and usage monitoring systems (HUMS), such as maneuver condition, order of execution, and pilot differences. Although a large database of flight recordings has been collected, these results focus on an overall analysis of planetary ring gear data that were recorded in two sets of flights. It is shown that variability due to torque is a major factor to be considered in real-time HUMS design and that certain steady state maneuvers yield a dramatically higher percentage of stationary recordings. Finally, it is conjectured that multi-axis recording may have previously unrecognized advantages for signal conditioning or analysis.

INTRODUCTION

A significant body of research exists concerning the vibration patterns of rotorcraft drive trains using test stand data [1-4], yet there is a dearth of results from data gathered in flight. A welcome exception is the work recently reported by Hess *et al* [5] involving the use of an SH-60 iron-bird ground simulator for comparison with test aircraft. While it would be desirable to apply engineering knowledge or test stand results directly to the flight situation, factors such as vehicle state, environmental conditions, and maneuvering forces can be expected to have important, yet poorly understood, effects on observed vibration patterns. Furthermore, many sources of aircraft vibration that are present in flight, such as the engine, main rotor, and tail rotor, make vibration recordings more difficult to analyze or interpret than those simply collected from isolated test rigs.

A continuing series of flight studies is being conducted at the NASA Ames Research Center (ARC) to collect reference data and to explore the extent of these effects. This paper reports on the analysis of vibration data collected from the first two-phase flight experiment that was completed in May 1999 on the Flying Laboratory for Integrated Test and Evaluation (FLITE), which is a Cobra AH-1 rotorcraft maintained by the US Army at Ames [6]. Specifically, this paper describes overall experiment-wide findings regarding the statistical stationarity of transmission vibrations during various maneuvering conditions, as well as the outcome of several analysis-of-covariance (ANCOVA) models. Although data were collected from three locations on the transmission during these

¹ Now located at Portland State University.

studies, these analyses are limited to those collected at a single planetary ring gear location. Analyses of data collected at the input pinion may be reported at a future time. To allow for the greatest research flexibility, vibration recordings were made using tri-axial accelerometers; hence, multi-axis vibration response characteristics are also reported.

OBJECTIVES

The present flight experiment was designed to determine the extent to which steady-state maneuvers influence characteristic vibration patterns measured at the input pinion and output planetary gear locations of a main helicopter transmission. The overall objective was to develop a better understanding of the manner in which several inter-related factors contribute to the size and variability of the vibration signals, and possibly to identify the most satisfactory flight conditions under which to acquire data for continuous on-board health monitoring applications.

As a whole, the research sought to determine if certain maneuvers systematically influence vibration patterns knowledge that might be used to detect and recognize aberrant signals associated with the growth of internal transmission damage. The study was also designed to collect a library of baseline flight data and to develop methods for comparison of flight data with those obtained from test stands at Glenn Research Center (GRC). Finally, because this was the first vibration study on the Cobra aircraft, considerable effort was invested in developing an in-flight recording apparatus, exploring accelerometer mounting methods, and generally learning about the overall vibratory characteristics of the aircraft itself.

METHOD

Aircraft Instrumentation

A data acquisition system designed specifically for this application (*HealthWatch*) was located in the tail boom and recorded eight-channels of analog data (Fig.1). Two three-axis Endevco model 7253A-10 accelerometers, denoted A and B, were positioned initially at the planetary ring gear (annulus) and input pinion gear locations respectively. The accelerometers were screw-mounted onto specially fabricated hexagonal brackets that were threaded onto existing transmission housing bolts (Fig. 2). In addition to the six accelerometer channels, one channel was used for sampling a once-per-revolution tachometer pulse from the main rotor shaft, using the aircraft's standard rotor track and balance equipment. The remaining channel was used for recording engine torque from a calibrated oil pressure transducer connected to the cockpit panel instrument.



Figure 1. HealthWatch flight module.



Figure 2. Triaxial accelerometer and mounting bracket.

Taking into account the resonant frequency of the accelerometer mounting bracket, which was analyzed to be 23kHz, an eighth-order, low pass anti-aliasing filter with a cutoff frequency of 18.432KHz was used in combination with a per-channel sampling rate of 50kHz to satisfy the Nyquist sampling conditions. In addition to analog data, time-correlated aircraft attitude information was also obtained from a MIL-STD-1553 serial data bus, which was updated at approximately 33Hz. The seven parameters used in this study included, radar altitude, airspeed, rate-of-climb, heading, bank angle, pitch angle, and side slip.

Accelerometer Validation and Gain Settings

During an early test flight prior to the main experiment, while maneuvers were being practiced, excessively high peak-to-peak g-levels ($-500g$) were observed at the pinion location. Such levels exceeded the dynamic range of the accelerometers and signal clipping occurred. Since published vibration levels were not found in the open literature for any helicopter transmission, there was concern initially that the observations were due to a recording artifact. Based on this, accelerometer B (channels 4-6) was moved to a new location at some distance from the mesh contact point of the input pinion where it was originally placed.

Table 1 compares the RMS values for a sample flight condition (i.e., the low-power forward descent maneuver) from the early test flight and three data records taken after accelerometer B was moved. There was a substantial 36% RMS reduction on channel five, which produced most of the signal clipping, accompanied by a tolerable RMS increase of 22% in channel four. While accelerometer B was mounted near the pinion gear during Phase 1, therefore, the gains on the signal conditioning board were set at $-250g$, except for channels four and five that were set at $-500g$. During Phase 2, when both accelerometers were positioned near the planetary ring gear, the gains were uniformly set at $-250g$.

Table 1: RMS (g-level) for forward descent maneuver during phase 1

Channel	Tri-Axial Accelerometer	Phase 1 Gain	Phase 2 Gain	Phase 1 Test Flight	Phase 1 Record 1	Phase 1 Record 2	Phase 1 Record 3
1	A	250	250	27.86	34.57	33.84	32.77
2	A	250	250	20.03	20.98	22.10	22.80
3	A	250	250	12.55	15.39	14.57	14.61
4	B	500	250	64.74	86.52	74.87	76.94
5	B	500	250	198.73	128.01	123.69	127.63
6	B	250	250	23.37	21.59	19.97	19.70

The conclusion that high g-levels are an inherent aspect of this Cobra transmission, and not an anomaly due to the data recording system, was further corroborated by an independent shake-table test. The highly consistent output of each accelerometer channel is shown for sine wave amplitudes of 30g (Table 2). In general, all channels were found to be highly linear and independent of each other up to this shake-table limit. The column labeled $RMS \times \sqrt{2}$ shows theoretical peak values for sine wave inputs, which conform closely to the observations. Hence, there was no reason to believe that the accelerometers or the data acquisition system would account for the high signal amplitudes observed in flight.

Table 2: Shake table results for 30g peak sine wave inputs

Channel	RMS	RMS $\times \sqrt{2}$	Peak
1	21.72	30.72	31.13
2	21.91	30.99	31.74
3	22.08	31.23	31.37
4	22.38	31.65	33.20
5	21.75	30.76	31.25
6	21.96	31.06	31.74

Experiment Design

The experiment was conducted in two phases, each composed of a set of four flights flown on successive days. Phase 1 was completed in Oct. 1998 and Phase 2 in May 1999. In each set of flights, the same two pilots flew the aircraft in various steady-state maneuvers (Table 3), according to a pre-determined test matrix (Table 4). This test matrix utilized a modified Latin-square design to counterbalance random wind conditions, ambient temperature, and fuel depletion [7].

At the start of each flight a recording was taken on the ground (Maneuver G) with the blades at flat pitch, and a second recording was taken in flight at low hover (Maneuver H). These and the 12 primary flight maneuvers were each scheduled to last 34 seconds in order to allow sufficient number of cycles of the main rotor and planetary gear assembly to apply candidate signal decomposition techniques to the recorded signals. In each phase of the experiment, therefore, 72 raw data records of 34 seconds were obtained for the primary test conditions: 12 maneuvers, flown by two pilots, on three separate occasions. Counting the 16 aggregate hover and ground recordings taken at the start and end of each flight, a grand total of 88 recordings were obtained per flight phase, or 176 recordings for the complete two-phase experiment. It may be noted that since each of eight analog channels was sampled at 50kHz, and correlated 1553 data were also taken from the bus, a massive amount of data was collected on each flight. This was stored on a high-density removable (Jaz) cartridge and removed at the end of the flight.

As mentioned above, during Phase-1, the two three-axis accelerometers, A and B, were mounted near the planetary ring and input pinion gears respectively. During Phase-2, the accelerometer near the input pinion (B) was moved to a new location at the planetary ring gear with appropriate changes made to the gains. In all respects other than the location of accelerometer B, the two phases of the experiment were conducted in exactly the same manner.

Table 3: Aircraft maneuvers for phases 1 and 2

Maneuver	Name	Symbol	Description
A	Forward Flight, Low Speed	FFLS	Fly straight, level, & forward at ~ 20 kts airspeed.
B	Forward Flight, High Speed	FFHS	Fly straight, level, & forward at ~ 60 kts airspeed.
C	Sideward Flight Left	SL	Fly straight, level, & sideward left.
D	Sideward Flight Right	SR	Fly straight, level, & sideward right.
E	Forward Climb, Low Power	FCLP	Fly forward, straight, & climb at 40 psi torque.
F	Forward Descent, Low Power	FDLP	Fly forward, straight, & descend at 10 psi torque.
G	Flat Pitch on Ground	G	Vehicle on ground skids.
H	Hover	H	Stationary hover.
I	Hover Turn Left	HTL	Level hover, turning left.
J	Hover Turn Right	HTR	Level hover, turning right.
K	Coordinated Turn Left	CTL	Fly level, forward, & turning left.
L	Coordinated Turn Right	CTR	Fly level, forward, & turning right.
M	Forward Climb, High Power	FCHP	Fly forward, straight, & climb at 50 psi torque.
N	Forward Descent, High Power	FDHP	Fly forward, straight, & descend at 50 psi torque.

Table 4: Flight protocol for each phase of experiment

		Obs. Order	Ground & Hover		Primary Flight Maneuvers						Hover & Ground	
Pilot 1	Flight 1	1	G	H	A	B	C	D	E	F		
		2			B	C	D	E	F	A		
		3			C	D	E	F	A	B	H	G
	Flight 2	1	G	H	I	J	K	L	M	N		
		2			J	K	L	M	N	I		
		3			K	L	M	N	I	J	H	G
Pilot 2	Flight 3	1	G	H	D	E	F	A	B	C		
		2			E	F	A	B	C	D		
		3			F	A	B	C	D	E	H	G
	Flight 4	1	G	H	L	M	N	I	J	K		
		2			M	N	I	J	K	L		
		3			N	I	J	K	L	M	H	G

RESULTS

Conceptual Causal Model

The analyses presented below were done within the notional framework of an open-loop causal model (Fig. 3). In this paradigm it may be noted that the various maneuvers, {M}, are thought to induce the set of observable aircraft attitudes, {A}, which induce potentially observable inputs, {I}, to the transmission. The internal responses, {R}, that occur within the transmission itself are not directly observable, but produce measurable outputs {O}. Other potentially measurable parameters within each set are italicized. Since it is assumed, by hypothesis, that the specimen aircraft had no transmission damage, the results presented here are considered determined by these causal relationships plus additional random or uncontrolled factors such as turbulence or other environmental conditions. If the transmission were damaged to some small extent, however, these effects would have been combined in some complex manner within the output set {O}. In a general sense, then, the knowledge gained from this kind of empirical research is hoped to separate what is predictable from what is not, and lay the groundwork for efficient detection of internal damage states.

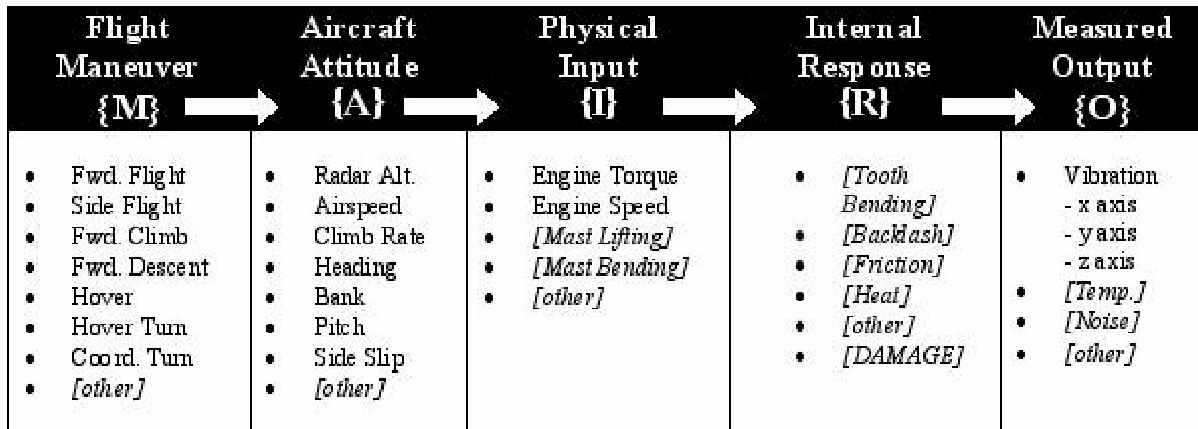


Figure 3. Conceptual open-loop model illustrating assumed causal relationships.

The Use of RMS for Assessing Vibration Responses

The univariate statistical analyses reported here use only the root-mean-square (RMS) of the vibration time series as the dependent variable, though considerable ongoing interest lies in isolating and identifying spectral patterns. The justification for using this simple property of the time-series is based on the insights provided by *Parseval's Theorem* [8]:

$$MS = (RMS)^2 = \mu^2 + \sigma^2 = \sum_{i=0}^{N/2} P_i$$
$$\mu^2 = P_0 = 0$$

where MS , μ and σ are the mean-square, mean, and standard deviation of the infinite time series, respectively, P_i is the power of the i^{th} frequency band in the periodogram, and $N/2$ is the number of bands. Since a vibration signal has a theoretical mean (or bias) of zero, it is evident by substitution that the mean-square is also equal to the series variance in the time-domain, or the total power in the frequency domain. Therefore, although in theory it is possible for the shape of the spectral distribution to remain constant while the overall RMS changes, this circumstance is very unlikely to occur in practice. In virtually all cases, observed differences will show concomitant changes in the spectral distribution that will also be observable using frequency or time-frequency analysis methods.

Data Reduction

To facilitate the statistical analyses, the data were reduced in two stages. Each stage produced highly compressed summary information, which has been archived as a derived database and is available for continued analyses. In the first stage, the basic statistical properties of each 34 sec. recording of raw flight data were consolidated into summary matrices (SMs). This was done entirely in the time domain by calculating the first four moments of each parameter, including the 1553 bus information, on a revolution-by-revolution basis. Because each recording had at least 178 revolutions, each SM, is a $178 \times p$ matrix, where the p columns contain the mean, and standard deviation or RMS of the various parameters for one shaft revolution. Since each shaft revolution took approximately 0.2 sec., and sampling occurred at 50 kHz, approximately 10,000 data points were compressed into each summary statistic in the SMs. The number of data counts for each revolution was also used to calculate an RPM measure of the rotor shaft, and included as a reference parameter. Since the flight attitude parameters were obtained from the 1553 bus at 33 Hz, significantly fewer data points went into these calculations. Nonetheless, they were averaged on a revolution-by-revolution basis and are quite suitable for examining functional relationships between the transmission's vibration output characteristics and the aircraft attitude state.

In order to perform analyses on an experiment-wide basis, the second stage of data reduction involved consolidating selected parameters into a single experiment data matrix (EDM), with groups of rows derived from the different SMs. Each row in the EDM is referred to as a case. Based on a preliminary analysis, it was decided that data collected from condition G, Flat Pitch on Ground, would be set aside for other uses, and was therefore eliminated. This reduced the number of SMs involved to 160. Since four hover recordings were made during each Phase, it was further decided to set aside the last hover for each pilot, so that each flight condition was uniformly represented by three ordered observations in the analyses. This reduced the number of SMs involved to 156. Finally, so as to obtain information reflecting time-series variability, summary statistics in the EDM were computed separately for each successive group of 28 revolutions, making a total of six ordered replications for each of the 156 SMs. The few extra revolutions in each SM were discarded. In addition, for each of the resulting $156 \times 6 = 936$ cases in the EDM, the average number of runs across the three axes above and below the 28 revolution median was also retained for testing stationarity of the acceleration and torque data [9].

Data Preparation

Principal Components Analysis

For research purposes, tri-axial accelerometers were used to obtain vibration data in three-dimensions. This allowed the flexibility of manipulating the recording axes analytically, and using multivariate statistics. Principal components analysis (PCA) is amongst the oldest and most widely used of multivariate techniques [10]. It is used to

describe the variation of the data in terms of a set of uncorrelated variables, called the *principal components* (PCs), each of which is a linear combination of the original variables. The procedure assures that, starting with the first, each successive PC captures the maximum amount of remaining variance, which is reflected in the normalized *eigenvalues* of the covariance matrix. Algebraically, given an m -dimensional data vector \mathbf{X} , which contains the original variables of interest, PCA decomposes \mathbf{X} as follows:

$$\mathbf{X} = \mathbf{S}\mathbf{P}^T = \sum_{i=1}^m s_i \mathbf{p}_i^T$$

where the \mathbf{p}_i are eigenvectors of the $m \times m$ covariance matrix of \mathbf{X} , and contain the weighting coefficients of the PCs. The s_i constitute the columns of the score matrix of the principal components, which contain the information about how the samples are clustered about the principal component axes. A geometric interpretation is illustrated in Figure 4, where the original observation axes (X,Y,Z) are rotated to the principal component axes (PC-1,PC-2,PC-3). Coordinate values for any point $P(x, y, z)$ correspond to point $P'(p1, p2, p3)$, which are the scores on the new principal component axes.

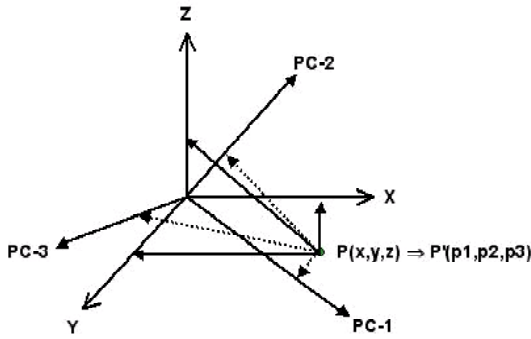


Figure 4. Principal components analysis transformation

The PCA transformation was done independently for each Phase of the experiment, treating the per-revolution RMS data as an aggregate, as opposed to each treatment separately. Following the description above, the first principal component PC-1 may be regarded as an optimal linear combination of the original RMS values, in the sense of accounting for the maximum amount of variability in three-dimensional space. Note that because the RMS was used the results do *not* correspond with optimal transducer mounting directions that might be computed from the raw acceleration data. Because RMS is the root of the signal *variance*, the natural logarithm of the data were computed prior to applying the PCA transformation in accordance with Scheff's [11] analysis-of-variance procedures for testing the equality of treatment variances rather than treatment means. Average PCA scores for each group of 28 revolutions were then saved in the EDM as individual cases, and are referred to as the PC-1, PC-2, and PC-3 scores. All subsequent statistical analyses were performed on these. In order to evaluate stationarity, the number of runs above and below the score medians for each axis were also saved in the EDM.

Stationarity Analyses

A major concern for meaningful analysis of vibration data is the extent to which the recorded time-series are *stationary* meaning, the extent to which the statistical properties of the series remain invariant over the recording interval. This issue is particularly relevant for planetary system monitoring, because it is necessary to record over long time periods (e.g., 30 sec. or more) to apply known decomposition algorithms. Nonstationarity in such signals, therefore, introduces the possibility of distorting the frequency content of the resulting signatures in a non-linear fashion.

In order to evaluate stationarity on an experiment-wide basis, a non-parametric runs test [12] was performed for each of the cases in the EDM. This test is equivalent to evaluating the probability of obtaining the observed number of runs from a sample of 28 observations from a binomial distribution with $p = 0.50$. Since there were 72 cases for each maneuver, a convenient overall figure of merit for maneuvering stationarity is the percentage of cases that were *not* found to be significant. As a cautionary note, therefore, the procedure equates stationarity with the null-hypothesis, which at best is inferred by the absence of a statistically significant result. Furthermore, the analysis only speaks to stationarity *within* sequences of 28-revolutions (i.e., cases), and not the longer 34 sec. recording periods. The study of stationarity within individual revolutions, or synchronously averaged revolutions, is the subject of time-frequency analysis [13-15], and outside the immediate scope of this paper.

Table 5 shows the percentage of stationary cases for time-series obtained from accelerometer A, located at the planetary ring gear during both phases of the experiment, i.e., channels 1-3. Based on inspection, one observation of Maneuver E, Pilot 2, (6 cases) was eliminated as an outlier. Hence, the total number of cases used was 630. The average percentage of cases that were stationarity is 68.58%. Since 72 tests were made in each instance, at the 0.01 level of significance, less than one significant finding would be expected purely on the basis of chance. It is clear, therefore, that these flight data contain a very high proportion of internally nonstationary records.

It is also apparent that nonstationarity was not the same across maneuvers. Several flight conditions, most notably forward and sideward flight, were severely nonstationary. Low- and high-power forward climb conditions, however, were highly stationary 98.48% and 91.67% respectively. It is speculated that this is due to a more constant disc loading during these maneuvers, which induced a relatively constant set of input forces to the transmission. Torque variability was also observed to be lowest during these maneuvers, a fact that is consistent with this reasoning. Maneuver G, flat pitch on the ground, although not shown in the table was 100% stationary.

Table 5: Stationarity based on runs tests for accelerometer A

MANEUVER	Count	Percent	Cases
A Forward Flight, Low Speed	45	62.50	72
B Forward Flight, High Speed	38	52.78	72
C Sideward Flight Left	30	41.67	72
D Sideward Flight Right	29	40.28	72
E Forward Climb, Low Power	65	98.48	66
F Forward Descent, Low Power	50	69.44	72
H Hover	64	88.89	72
I Hover Turn Left	58	80.56	72
J Hover Turn Right	42	58.33	72
K Coordinated Turn Left	45	62.50	72
L Coordinated Turn Right	56	77.78	72
M Forward Climb, High Power	66	91.67	72
N Forward Descent, High Power	48	66.67	72
AVERAGE		68.58	

($\alpha = .01$)

Comparisons using Multiple Regression and Analysis-of-Covariance

Multiple regression analysis is concerned with estimating the functional relationship between a group of predictor variables and a single dependent variable. In this instance the aircraft attitude measures were used as linear predictors of PC scores. In general, if the means of subgroups in an experiment are greatly different, the variance of the combined groups is much larger than the variances of the separate groups. Analysis-of-variance (ANOVA) methods, which specifically address differences in subgroup means, are based on this fact [7, 16]. In this study, a fixed-effects analysis-of-covariance (ANCOVA) was used, which combines the properties of both multiple regression and ANOVA. In effect, it was used to determine the differences in score means between the various treatment categories, as well as the degree to which the covariates, i.e., flight parameters, influenced total variability. A *fixed-effects* model was used because none of the experimental factors, possibly with the exception of pilots,

was randomly sampled from a larger population to which generalizations would be meaningful. An attractive feature of this approach is that it partitions the total sum-of-squares (Total SS) around the global mean of the experiment, on an additive basis. This partitioning is useful for assessing the relative contribution of the measured covariates versus the category factors, as follows:

$$\text{Total SS} = \text{Covariate SS} + \text{Main Effects SS} + \text{Interaction SS} + \text{Error}$$

Referring to the causal model described in Figure 3, it would have been desirable to have direct measures of all *essential* inputs $\{I\}$ to the transmission. Unfortunately, it is still largely a matter of conjecture as to what this basic set might be, and of those suggested in the diagram only engine torque was measured directly. Based on observations made during the stationarity analysis, however, it was postulated that the flight parameters should correlate with transmission input forces, particularly those that might have a direct relationship to mast lifting or bending. For this reason, the recorded flight parameters were treated as covariates. Since the three principal component scores are uncorrelated, and might possibly yield different insights into the nature of transmission vibrations in three-dimensional space, separate analyses were conducted for each of them. Finally, based on an initial exploratory analysis, it was decided to retain only two-way interaction terms and pool the higher-order interactions within the residual error.

In the hierarchical version of ANCOVA that was used here, the linear regression of the covariates is removed first. This makes the analysis identical to first performing a standard multiple-regression analysis using the covariates as predictor variables, and then performing a simple ANOVA on the residual. The three regression analyses for the principal component scores are summarized in Table 6. These will be discussed in conjunction with the main ANCOVA, which also summarizes analyses of each of the three principal component scores (Table 7). In both tables the F-ratios are omitted because they can be reconstructed from the data, and an asterisk indicates whether the effect is significant at the 0.01 level of confidence.

Table 6: Multiple regression and beta weights for aircraft attitude on three principal component scores

	PC-1	PC-2	PC-3
R	0.956 *	0.528 *	0.140
R Square	0.914	0.279	0.020
Variable $\{A_i\}$	Beta	Beta	Beta
Airspeed	0.042 *	-0.050	0.053
Altitude	0.013	-0.039	0.047
Bank Angle	-0.016	0.036	-0.034
Heading	-0.036 *	0.103 *	0.019
Pitch Angle	-0.060 *	-0.278 *	0.103
Climb Rate	0.041	-0.570 *	-0.074
Rotor RPM	0.017	0.138 *	-0.078
Torque	0.958 *	0.556 *	-0.032

* significant at $\alpha = 0.01$

Interpretation of Results

Regression Analyses

The most striking aspect of the combined analyses is the massive amount of experimental variance accounted for by torque 91.4% for PC-1 scores (Table 6). This was not completely unexpected considering many earlier results obtained from test-rigs [4], but it is still impressive. In Table 6, the square of the regression coefficient (R Square), is a measure of explained variance, which is the same as the Percent Total SS attributed to covariates seen in

Table 7. It is interesting to note that the R Square of torque drops to 27.9% for PC-2, and has only 2% predictive value for PC-3.

Beta coefficients shown in Table 6 are the weights calculated by least-squares for the three standardized multiple regression equations. Standardizing transforms the variables into standard deviation units from their respective sample means, and is an effective procedure for understanding the relationships between factors that were not measured in the same units. Symbolically,

$$PC_i = \sum_{j=1}^k \beta_{ij} A_{ij} + c_i$$

where the β -coefficients weight the aircraft attitude parameters $\{A_j\}$ for linear prediction of the i^{th} principal component, with c_i as the intercept.

With regard to the PC-1 regression equation, therefore, torque has the largest predictive weighting (0.96) and the other flight variables are almost equally represented at very low levels. However, for the PC-2 regression equation torque weighting diminishes (0.56) and rate-of-climb takes on an equally important predictive role (0.57). Pitch angle and rotor RPM also increase in relative importance. Thus, it may be concluded that the first two principal components reflect somewhat different vibration effects. The flight parameters have almost no predictive relationship to PC-3, which of course has a very small amount of total variance.

Principal Component Comparisons

Before proceeding with a discussion of individual category effects in the analysis-of-covariance (Table 7) it is interesting to note that once covariate regression is removed, PC-1 and PC-2 retain similar amounts of variability to be distributed between the main effects and 2-way interactions. Rotating the original coordinates by PCA, in effect, brings about a consolidation of most of the torque-induced vibration energy onto PC-1 (90.66%). PC-2 primarily accounts for *main effects* variance (63.80%), and PC-3 for *2-way interaction* variance (32.57%). On a general basis, therefore, it would appear that PCA systematically shifts higher-order interactions to the higher principal components. In view of the fact that the PCA procedure places the largest remaining variance on each axis, this is understandable: PCA and ANCOVA are simply two different ways of partitioning total variance. In this experiment, since a greater percentage of variability is associated with covariates than with main effects, this is reflected onto the first principal axis. Since greater variability is also associated with main effects than with 2-way interactions, this is reflected onto the second axis, and so forth. Finally, it may be noted that the percentage of residual (i.e., unexplained) variability systematically increases from PC-1 (2.59%) to PC-3 (46.82%), indicating that PC-3 scores are largely, although not completely, random noise.

Table 7: ANCOVA partitioning of sum of squares for each principal component

Source of Variation	PC-1				PC- 2				PC- 3	
	df	Sum of Squares	Percent Total SS		Sum of Squares	Percent Total SS		Sum of Squares	Percent Total SS	
Covariates	8	558.778	91.40	*	10.977	27.85	*	0.018	1.97	
Torque	1	554.282	90.66	*	0.007	0.02		0.003	0.33	
Rate of climb	1	0.552	0.09	*	7.690	19.51	*	0.000	0.00	
Pitch angle	1	2.832	0.46	*	2.028	5.15	*	0.003	0.33	
Airspeed	1	0.165	0.03	*	0.061	0.15	*	0.001	0.11	
Altitude	1	0.030	0.00		0.095	0.24	*	0.003	0.33	
Bank angle	1	0.125	0.02		0.214	0.54	*	0.002	0.22	
Heading	1	0.643	0.11	*	0.221	0.56	*	0.001	0.11	
Rotor rpm	1	0.148	0.02	*	0.661	1.68	*	0.005	0.55	*
Main effects	21	27.497	4.50	*	25.143	63.80	*	0.171	18.75	*
Maneuver	12	26.092	4.27	*	24.938	63.28	*	0.139	15.24	*
Order	2	0.504	0.08	*	0.010	0.03		0.017	1.86	*
Pilot	1	0.024	0.00		0.185	0.47	*	0.003	0.33	
Phase	1	0.818	0.13	*	0.000	0.00		0.004	0.44	*
Replication	5	0.059	0.01		0.010	0.03		0.007	0.77	
2-way interactions	133	9.239	1.51	*	1.313	3.33	*	0.297	32.57	*
Maneuver X Order	24	4.771	0.78	*	0.425	1.08	*	0.047	5.15	*
Maneuver X Pilot	12	1.254	0.21	*	0.134	0.34	*	0.098	10.75	*
Maneuver X Phase	12	0.823	0.13	*	0.529	1.34	*	0.071	7.79	*
Maneuver X Replication	60	1.014	0.17		0.133	0.34		0.051	5.59	*
Order X Pilot	2	0.119	0.02		0.012	0.03		0.000	0.00	
Order X Phase	2	0.133	0.02		0.007	0.02		0.007	0.77	*
Order X Replication	10	0.126	0.02		0.014	0.04		0.006	0.66	
Pilot X Phase	1	0.204	0.03	*	0.017	0.04		0.005	0.55	*
Pilot X Replication	5	0.098	0.02		0.012	0.03		0.004	0.44	
Phase X Replication	5	0.030	0.00		0.025	0.06		0.006	0.66	
Explained	162	595.514	97.41		37.433	94.99		0.485	53.18	
Residual	767	15.858	2.59		1.976	5.01		0.427	46.82	
Total	929	611.371	100.00		39.409	100.00		0.912	100.00	

* significant at $\alpha = 0.01$

With regard to treatment main effects and two-way interactions, there is good reason to be interested in all of them, but for somewhat different reasons. It was expected, of course, that maneuvers would differ in vibration pattern. This is supported by the fact that maneuver is the strongest overall main effect for the three principal components, accounting for 94.9%, 99.2% and 81.3% respectively of their main effects sum-of-squares. It should be emphasized that these and other differences were obtained after the combined effects of the aircraft attitudes {A} were removed.

The order of observation of the maneuvers was found to be significant in PC-1 and PC-3, but accounted for only a small percentage the total variance. This factor is interesting because fuel depletion systematically lowers the gross weight of the vehicle after each observation during the flight. Based on the current findings, it is probably not a highly critical factor within the range of weight changes that occurred. There is some suggestion, however, that gross-weight might be a factor in future HUMS.

The pilot factor is statistically interesting for several reasons. First, as one would expect, the two well-trained test-pilots performed individual maneuvers somewhat differently, while not differing substantially on an overall basis. Although the pilot main effect is only significant on PC-2, the pilot-maneuver interactions are significant for all three components, indicating that some maneuvers were performed differently than others. Essentially, these differences tended to balance out and do not appear as significant main effects for PC-1 or PC-3. It should be noted, of course, that although a very small amount of total variability is accounted for by these pilot differences, it would have been highly suspect not to find any at all because maneuvering control was completely in their hands. What is surprising, and rather encouraging for HUMS applications, is that pilot differences were so *small* relative to the observed differences in maneuvering and other treatments.

A small but significant main effect of experiment phase is found on PC-1 and PC-3. Significant interactions between phase and pilot on PC-1 and PC-3 also indicate pilot differences between the two phases of the experiment. It is not clear whether these effects were due to time of year, temperature differences, climactic variations or simply modifications in how the pilots went about their flying tasks.

Finally, the replication variable uniformly has no significant main effect on the three PC scores. A small interaction effect with maneuver is found on PC-3, however, which possibly suggests some form of trend difference between the time series obtained on different maneuvers. Overall, this is an agreeable result showing that the order of the six cases within each 43 sec. recording period had little or no effect.

DISCUSSION AND CONCLUSIONS

This paper has analyzed flight data from an AH-1 Cobra helicopter to evaluate the relative importance of several operational factors that are thought to impact the effectiveness of onboard transmission vibration monitoring systems. These included maneuvering states, aircraft attitudes, pilot differences, temporal changes, and data replications. The methodological value of obtaining such experimental data has been amply demonstrated. Based on lessons learned from the current study, an OH-58C helicopter at Ames has been similarly instrumented and data have been collected using the same flight-test protocols. Specific comparison studies between the two aircraft will be reported at a future date, as well as comparisons with data collected from NASA Glenn's 500 HP OH-58C test facility [4, 17, 18].

From the perspective of effective transmission monitoring, this study draws attention to the important fact that in-flight vibrations are, to a very large extent, dominated by torque and torque variability. As a consequence, successful monitoring algorithms must overcome the challenge of identifying small diagnostic signatures, reflecting internal damage states, well before component destruction becomes so dramatic as to outweigh the dominant torque effects. In order to do this, effective means must first be found to prepare the incoming raw data to take these effects into account. This might be approached in several ways based on a more thorough exploration of the non-linear relationship between torque and the vibration signal.

Although the present findings require further validation on other aircraft, of the several maneuvers investigated here, forward climb conditions produced stationary signals with the greatest consistency. It is conjectured that this finding was mediated by torque constancy, but it is doubtful that climbing maneuvers *per se* are feasible conditions for restricting real-time HUMS analysis. Again, the solution to utilizing data from random flight states lies in having a much better understanding of the relationship between torque and the vibration signal itself.

Although the use of tri-axial accelerometers was originally intended to provide maximum research flexibility, e.g., to synthesize single-axis accelerometers in various angular orientations, the present findings suggest other practical uses for them. For example, in a torque-based environment it is clearly desirable to separate torque effects as discussed above. This could be achieved by measuring torque directly, as was done here, and then applying some form of linear or non-linear regression to produce a residual signal for analysis. Intriguingly, it might also be achieved by recording from tri-axial accelerometers, rotating to principal components, and then using the higher components for signal analysis. As will be recalled, the effects of torque were largely consolidated onto the leading principal component. Whether this conjecture is valid or valuable is being explored in the laboratory along with other possibilities.

Finally, it should be mentioned that during the course of this study it has become even more evident that internal transmission component failures can only be observed systematically in ground-test facilities. For this reason, signal detection algorithms must necessarily be developed, and evaluated in those environments, particularly to establish their potential hit-rate ability. Permanently instrumented research aircraft, such as NASA's Cobra, OH-58C, and UH-60 helicopters, however, are also needed to evaluate equally important false-alarm rates under the full range of normal operating conditions.

Acknowledgments

The authors would like to express their gratitude to Mr. Larry Cochran, Sigpro, for aircraft instrumentation and raw data reduction, and, Ms. Alissa Fitzgerald, of the same organization, for her engineering design and analysis of the accelerometer mounting brackets used in this study.

REFERENCES

1. Hollins, M.L., *The Effects of Vibration Sensor Location in Detecting Gear and Bearing Defects*, . 1986, Naval Air Test Center: Patuxent River, MD.
2. Chin, H., K. Danai, and D.G. Lewicki. *Fault Detection of Helicopter Gearboxes Using the Multi-Valued Influence Matrix Method*. in *ASME Winter Annual Meeting*. 1993. New Orleans: American Society of Mechanical Engineers.
3. Hollins, M.L., *Test Bed Defective Component Data*, . 1991, Naval Air Test Center: Patuxent River, MD.
4. Zakrajsek, J.J., *A Review of Transmission Diagnostics Research at NASA Lewis Research Center*, . 1994, NASA Lewis Research Center: Cleveland.
5. Hess, A., B. Hardman, and C. Neubert. *SH-60 Helicopter Integrated Diagnostic System (HIDS) Program Experience and Results of Seeded Fault Testing*. in *American Helicopter Society 54th Annual Forum*. 1998. Washington: AHS.
6. Huff, E.M., et al. *Experimental Analysis of Steady-State Maneuvering Effects on Transmission Vibration Patterns Recorded in an AH-1 Cobra Helicopter*. in *American Helicopter Society 56th Annual Forum*. 2000. Virginia Beach: American Helicopter Society.
7. Hays, W.L., *Statistics for Psychologists*. 1963, New York: Holt, Rinehart and Winston. 719.
8. Oppenheim, A.V., A.S. Willsky, and I. Young, *Signals and Systems*. 1983, Englewood Cliffs, NJ: Prentice-Hall.
9. Bendat, J.S. and A.G. Piersol, *Random Data Analysis and Measurement Procedures*. 1986, New York: Wiley. 566.
10. Everitt, B.S. and G. Dunn, *Applied Multivariate Data Analysis*. 1991, New York: Wiley.
11. Scheff, H., *The Analysis of Variance*. 1959, New York: Wiley. 477.
12. Siegel, S., *Nonparametric Statistics for the Behavioral Sciences*. 1956, New York: McGraw-Hill. 312.
13. Forrester, B.D., *Gear Fault detection Using the Wigner-Ville Distribution*. *Mechanical Engineering*, 1991. **16**(1): p. 73-77.
14. Hambaba, A., E.M. Huff, and U. Kaul. *Detection and Diagnosis of Changes in the Time-Scale Eigenstructure for Vibrating Systems*. in *IEEE Aerospace Conference*. 1999. Blue Sky, Montana.
15. Robinson, T.W., et al. *Search for an Improved Time-Frequency Technique for Neural Network-Based Helicopter Gearbox Fault Detection and Classification*. in *World Conference on Neural Networks*. 1994. San Diego, CA: INNS Press Lawrence Erlbaum Associates.
16. Dixon, W.J. and F.J. Massey, *Introduction to Statistical Analysis*. 1957, New York: McGraw-Hill.
17. Lewicki, D.G. and J.J. Coy, *Vibration Characteristics of OH-58A Helicopter Main Rotor Transmission*, 1987, NASA Lewis Research Center: Cleveland.
18. Huff, E.M., et al. *Experimental Analysis of Mast Lifting and Bending Forces on Vibration Patterns Before and After Pinion Reinstallation in an OH-58 Transmission Test Rig*. in *American Helicopter Society 56th Annual Forum*. 2000. Virginia Beach: American Helicopter Society.